

# Numerical modelling of LCD electro-optical performance

H. WÖHLER<sup>1</sup> and M.E. BECKER\*<sup>2</sup>

<sup>1</sup>Autronic-Melchers GmbH, 18 Rosweid Str., D-76229 Karlsruhe, Germany

<sup>2</sup>Display-Metrology & Systems, 44 Marie-Alexandra Str., D-76135 Karlsruhe, Germany

*Realisation of complex high information density LCDs and systematic optimisation of their electro-optical and ergonomic performance would not be possible in the required time-frame without reliable numerical modelling of the electro-optical performance of such display devices. In this paper, we outline the history of numerical LCD modelling starting with Berreman and van Doorn, finally arriving at modern state-of-the-art LCD-modelling in two and three dimensions.*

*Numerical modelling of LCDs is carried out in two steps: first, the effect of the electrical field on the orientation of the liquid crystalline alignment has to be evaluated before the corresponding optical properties can be computed. Starting from LC-elasticity theory we present suitable numerical methods for computing various states of LC-deformation (stable, metastable, bistable, etc.) in one-dimensional problems.*

*Light propagation in layered anisotropic absorbing media is evaluated with the methods that are based on Maxwell's equations (Berreman 4×4-matrix approach). This approach can be simplified to yield methods with reduced computing time and sufficient accuracy for many problems (e.g. extended Jones 2×2-matrix formalism).*

*In two- and three-dimensional problems, i.e., in cells with lateral dimensions comparable to the cell thickness, a variety of different director configurations are possible for a given geometry and electrical driving and addressing, making the modelling more complicated. Moreover, local defects can occur, which should be also considered in the simulation. Suitable approaches for the director field calculation, i.e. the vector and the tensor approach, are discussed.*

*The complexity of the problem increases considerably when a third dimension is added, e.g. the geometry of the problem has to be defined in three dimensions together with the respective boundary conditions (anchoring geometry and elasticity) and electrodes. If strong deformations or even distortions are present in the orientation of the LC-layer, the applicability of known one-dimensional approaches for computing the optical properties must be checked and new approaches eventually have to be developed. The third dimension prohibits the use of some standard methods (e.g. FDTD), solely because of the enormous memory requirements and the long calculation times. Other approaches are presented and discussed.*

**Keywords:** LC-deformation, LC-optics, one-dimensional solution.

## 1. Introduction

The simulation of liquid crystal display devices (LCDs) via numerical modelling has become an indispensable part of the research and development of new electro-optical effects in LCs (i.e. development of novel display types) and of the optimisation of existing display effects, because it allows exact and individual control of all model parameters, fast results and thus it ideally parallels the laboratory workbench. Complex optimisation schemes can be used together with the numerical model in order to find special parameter combinations and to analyse parameter sensitivities. Numerical modelling of LCDs was successfully employed by van Doorn [1] and Berreman [2] in 1975 to explain the “bounce” in the dynamical optical response of TN-cells. At the time of its release in 1987 DIMOS was the first commercial software package for numerical modelling of display systems with LCDs [3].

Depending on the complexity of the display and on the targets of optimisation, the simulation effort can be as small as typing in a few numbers into a pocket calculator (e.g. transmittance of a TN-cell at normal incidence in the quiescent state) or on the other hand it requires high-end PCs or even workstation computers when lateral effects cannot be neglected as in the case of high resolution TFT-LCDs or in devices using the in-plane-switching (IPS) effect.

The LCD is composed of plane parallel layers like glass substrates, LC layer, polarises etc. As long as the lateral extensions are much larger compared to the thickness of the individual layers and if sufficient homogeneity of the material and cell parameters along the surface can be assumed, a one-dimensional model is the adequate approximation. In this case the LCD model is composed of layers with infinite lateral extension. Refractive indices and the director orientation vary only along one direction, usually the LCD normal. The amount of numerical calculations for the determination of the director configuration and the optical

\* e-mail: m.becker@display-metrology.com

quantities like transmittance and reflectance is moderate compared to two- or three-dimensional problems. This simple model allows performance optimisation with simultaneous variation of several material and cell parameters.

High-resolution displays with small pixels require two- or three-dimensional modelling, since “fringing field” effects cannot be neglected. As a result the director orientation may depend strongly on the lateral position. LCDs using the IPS effect carry electrodes on one substrate only, in contrast to the usual TN or STN-LCDs. The electric field in IPS-LCDs strongly depends on the position within a plane defined by the LCD-normal and a lateral direction, so that a two-dimensional model is required.

## 2. LC-deformation

Before we can calculate the optical properties of LCDs we must know all parameters describing the model and thus entering into the computation. These comprise the refractive indices, layer thickness and optic axis orientation in case of birefringent materials. The most problematic parameter is the orientation of the optic axis within the LC-layer.

On the molecular level the nematic liquid crystal is composed of rod-like molecules with the long axes of neighbouring molecules aligned approximately parallel to one another. The deviation from an ideal parallel alignment is due to thermal fluctuations of the molecules. The director, represented by the unit vector  $\vec{n}$ , is the temporal average of the molecular axes over a small volume at any location within the liquid crystal. The orientation of the director is allowed to change continuously within the medium, except at singularities, where the distances over which orientational changes occur are no longer much larger than the molecular dimensions.

In the following we use the term director rather than optic axis when considering LC-materials. The orientation of the director across the LC-layer as a function of the position is described by the director field. The director orientation is imposed only at the substrates due to a special treatment of the surfaces. However the orientation within the bulk of the LC-layer is not directly available in the general case. Oseen, Frank, Leslie, Ericksen, and others developed the theory of LC-elasticity [4–7]. This theory is the basis for the calculation of the director orientation within the bulk of chiral-nematic LC-materials.

Alternatively, the free energy of the liquid crystal can be written in terms of the order parameter tensor  $Q$ . This “tensor approach” maintains the physical equivalence of  $\vec{n}$  and  $-\vec{n}$  and is thus sometimes believed to be more “realistic” in the numerical modelling of LCDs. However, this approach can give rise to spontaneous transitions between topologically nonequivalent states without the generation of disclinations (e.g. inversion walls), solely based on discretisation, which is unrealistic from the viewpoint of LC-physics [8].

The vector approach will not calculate the energy of a disclination correctly, but it will qualitatively yield increasing energy with increasing deformation while the tensor method may eventually slip into a topologically non-equivalent configuration with lower energy. The transition into a non-equivalent state depends strongly on the grid spacing. It should be noted however, that in cases where defects exist, the basic assumption of LC-continuum theory collapses, i.e. that changes in director orientation are on scales much larger than the molecular dimensions.

Moreover, the mathematics involved in the vector approach is simpler, it requires fewer grid points for a given error, and the computing speed is higher.

### 2.1. Energy densities

The theory of elasticity provides expressions for the elastic energy density of an LC layer:

$$f_k = \frac{1}{2} \mathbf{K}_1 (\text{div } \vec{n})^2 + \frac{1}{2} \mathbf{K}_2 \left( \vec{n} \cdot \text{curl } \vec{n} + \frac{2\pi}{p_0} \right)^2 + \frac{1}{2} \mathbf{K}_3 (\vec{n} \times \text{curl } \vec{n})^2 \quad (1)$$

where  $\mathbf{K}_1$ ,  $\mathbf{K}_2$ , and  $\mathbf{K}_3$  are the elastic constants,  $p_0$  is the helical pitch. The coupling of the molecules with the electric field caused by an applied voltage is given by the electrostatic energy density:

$$f_e = \frac{1}{2} \vec{E} \cdot \vec{D} = \frac{1}{2} \vec{E} \cdot \epsilon \cdot \vec{E}. \quad (2)$$

The energy of the LC-layer is obtained by integration over the elastic and electrostatic energy densities. If there is significant elastic coupling of the molecules at the surfaces the surface energy must be added to the total energy. The energy acts as a starting point for the calculation of the director configurations.

**Surface energy.** Several expressions exist for description of a surface energy [9]. The commonly used approach was published by Rapini and Papoular [10]:

$$F_s = \frac{C}{2} \sin^2(\alpha - \alpha_s), \quad (3)$$

with the surface coupling parameter  $C$ . The treatment of the substrates produces a preferred direction of the molecules at the aligning layer surface. The tilt angle  $\alpha_s$  of the preferred direction is also called the pretilt angle (or tilt-bias angle). Torques from the bulk can reorientate the director at the aligning surface when the anchoring of the molecules is not infinitely strong. In this case we have an elastic coupling which is described by the surface energy.

**Dissipation function.** The modelling of the time dependent behaviour of the LC-layer requires additional expressions. These are the dissipation functions, which take into account the energy dissipation due to internal friction [11].

## 2.2. Stable configurations

When a constant voltage or a constant charge is applied to the LC-layer, the director relaxes from an initial configuration to a stable equilibrium configuration, which is characterised by the minimum of the total energy. In the case of constant charge ( $D_z = \text{const.}$ ) stable director configurations are given by minima of the Helmholtz-energy

$$W_H = \iiint f_k + f_\varepsilon d\mathbf{v} + F_s, \quad (4)$$

while at constant voltage the Gibb's-energy

$$W_G = \iiint f_k + f_\varepsilon d\mathbf{v} + F_s \quad (5)$$

must be minimised. The necessary condition for a stable equilibrium state is that the first variation vanishes. This yields the Euler differential equations for the unknown tilt and twist functions. It can be shown that the Euler equations derived from  $W_H$  and from  $W_G$  are identical [12,13]. Thus calculating equilibrium states means either minimisation of the total energy of the system or solving the Euler equations.

**Calculating stable configurations.** Apart from a few simple cases the director configurations must be calculated numerically. This can be done either by numerical integration of the differential equations or by using a suitable relaxation method. The latter class of methods also allows the simulation of the time dependent behaviour in a natural way by use of adequate dissipation functions. The relaxation methods start with an initial director configuration, which is either a previously calculated equilibrium state or just a first guess. Then in a first step, a new, more relaxed configuration is calculated using equations derived from the discretised differential equations or the discretised energy expression. This process is repeated until the newly computed configurations do not show significant changes. Then, an equilibrium state is reached. A suitable discretisation of the differential equations or the energy is crucial for efficient calculation of director states. Discretisation means that the unknown function describing the director configuration (e.g. tilt and twist angle) are replaced by piecewise defined, in general simple functions (often linear). As long as they are well chosen and the distance over which they are defined is small enough, good approximations can be obtained. The parameters of the approximating functions are then varied until an equilibrium state is reached. The parameters are often expressed as functional values at certain (discrete) positions in space and time.

## 2.3. Dynamic behaviour

When a voltage is switched ON or OFF or when a sequence of different voltage levels is applied e.g. in multiplex operation, the director configuration changes and tries

to approach the steady-state corresponding to the actual voltage level. Since nematic LCs are viscous fluids it is necessary to know at least the rotational viscosity for simulation of the dynamic behaviour. More detailed modelling includes lateral flow-effects in the LC-layer for which also the shear viscosity coefficients have to be known. If a relaxation method is used with the dissipation functions involving the viscosity parameters, the time dependent director configurations can be computed on a physical time-scale. The relaxation process then generates a sequence of director configurations, where each configuration corresponds to a certain moment in time.

## 2.4. Uniqueness of the director configuration

The equations for determination of the director configurations are nonlinear. This gives rise to multiple solutions for the director field describing the director configuration at certain voltage levels. Highly twisted STN-LCDs for example can show a small voltage range close to the threshold where bistability exists. Zero-field bistability effects with infinite holdingtimes are promising candidates for LCDs in mobile battery operated applications.

## 3. LC-optics

Up to now, we considered only the LC-layer between the alignment layers and the conductive layer. An electro-optical effect, visible for the human eye can only be achieved if either dichroic dyes are added to the LC-material or alternatively when sheet polarisers are attached to the LC-cell in order to obtain changes in light intensity (the human eye is not sensitive to changes of the polarisation state caused by the voltage induced reorientation of the LC-layer). The amount of light reflected and transmitted by LCDs depends on the wavelength and the direction of light propagation. These often undesirable effects can be reduced by additional optical elements like retarder sheets or a second compensating LC-layer. The modelling of the optics of LCDs must therefore take into account the multilayer stack character of the LCD and must also include the modelling of the single LC-layer, polariser, retarder, glass, alignment layer, and (transparent) conductive layer.

The optical model of the LC-layer is an inhomogeneous uniaxial medium, where inhomogeneous means that the orientation of the director (= local optic axis) varies in space. Addition of dichroic dyes to the non-absorbing LC-material is taken into account by the imaginary parts of the refractive indices.

A simple but in most cases sufficient model for the polariser is a uniaxial medium with different imaginary parts. They are responsible for the propagation and polarisation direction dependent extinction of the passing light wave. The real parts of the refractive indices are less important and can be set alike. The optic axis lies in the plane of stratification.

Retarders in contrast to polarisers have different real parts of the refractive indices. The absorption can often be neglected. The retarders can also be biaxial [14,15].

The other layers mentioned above can be treated as isotropic layers, eventually with absorption (e.g. glass substrates, ITO electrode, etc.).

## 4. One-dimensional solutions

If the thickness of the LC-layer is small compared to its lateral extensions, the one-dimensional model is sufficient. Even if this condition is not fulfilled, the one-dimensional simulation can give at least an idea of the basic electro-optical behaviour.

In the following we present methods for calculations of static and dynamic director configurations and methods for calculation of the optical quantities of interest.

### 4.1. LC-deformation

**Integration methods.** Integration methods are useful when “hunting” for static director configurations [16]. The problem can be described by two Euler differential equations and the boundary conditions for both alignment layers, so that it is mathematically a boundary value problem. The task is to fulfil the differential equations within the bulk and also the boundary conditions at the same time. In order to do that, one can replace the boundary value problem by an initial value problem. Numerical integration starts from one side of the LC-layer with the boundary conditions fulfilled on that side. The integration is done over the layer with an initial guess for some other integration parameters (i.e. “shooting”). The integration parameters are systematically varied until the boundary conditions are fulfilled on both sides.

**Relaxation methods.** Relaxation methods belong to the other class of methods. Either the energy of the LC or the corresponding Euler differential equations are discretised in the first step. For that it is necessary to find a suitable representation of the director  $\vec{n}$ . A natural representation is given by two angles, the tilt angle  $\theta$  and the twist angle  $\phi$ . Alternatively the director can be expressed by its three Cartesian components  $n_x$ ,  $n_y$ , and  $n_z$ . The discretisation subdivides the LC-layer into a sufficiently large number of sublayers so that the unknown functions describing the director configuration (i.e. tilt and twist or cartesian components) are locally well approximated by suitable simple functions (e.g. linear functions). The variable parameters are then given by the function values at the interfaces between adjacent sublayers, and usually replacing the spatial derivatives by differences of these function values. Discretising every sublayer results in a set of nonlinear equations for the function values at distinct locations.

The relaxation method generates a new director configuration in each iteration step. The dissipation functions mentioned above include derivatives of the director components (or tilt and twist angles) with respect to time. Suit-

able discretisation in time results in director configurations at a new time step. A simple discretisation scheme is “forward Euler”, with the time derivative replaced by a simple difference. This method however is not very accurate and more important it is numerically unstable which means that time step must be kept very small to avoid artifacts like oscillations in the director configurations. The so-called implicit or semi-implicit discretisation schemes require much more numerical calculations for each iteration step but they are numerically stable. Larger steps are possible so that the additional calculations are more than compensated.

It should be stressed that a proper discretization is crucial for the accuracy of the method. The advantage of the commonly used cartesian component representation is the simplicity of the expressions of the Euler equations or energy. Moreover they are more accurate in the high tilt region than the tilt and twist representation with a spatially linear approach. However the approach is less elegant since 3 rather than the 2 variables, necessary for describing the director, are used. Equations for all 3 components must be applied for the next iteration step so as if the 3 components were independent. Thus after every iteration step a normalization of the director is necessary. Moreover the condition  $|\vec{n}| = 1$  is only fulfilled at the interfaces between the sublayers and not within the sublayers. On the other hand the problems of the tilt and twist representation in the high tilt region can be solved by suitable nonlinear functions.

Dissipation functions do not necessarily define the relaxation method. Less physical methods like the Newton-Raphson method or the related Levenberg-Marquardt method can be applied [17–19]. They require additional information derived from the Euler equations or energy expressed as Jacobian matrix or Hesse matrix. These methods converge rapidly to the equilibrium state, but the director configurations generated through the iteration process cannot be associated with any time level, except for the equilibrium state, which corresponds to  $t \rightarrow \infty$ .

**Graphical representation of the director configuration.** The midplane tilt angle  $\alpha_m$  is a scalar quantity, which can represent the deformation of symmetric LCDs (same tilt angle on both substrates) quite well.  $\alpha_m$  as a function of the applied voltage (also called electro-distortional curve, Ref. 20) shows important characteristics like threshold voltage (voltage level where  $\alpha_m$  increases rapidly) and steepness (Fig. 1).

**Electro-optical characteristics.** Highly multiplexed LCDs require a steep electro-optical curve, which implies a steep electro-distortional curve. This can be achieved with higher twisted LCDs, the STN-LCDs (Fig. 2). A suitable choice of material parameters can further improve the steepness. Very highly twisted LCDs like the 270° cell show even bistability in a small voltage range which means two stable equilibrium states are possible at a given voltage. S-shaped electro-distortional curves indicate such a bistability. Another parameter, which strongly influences the steepness, is the surface coupling elasticity [21].

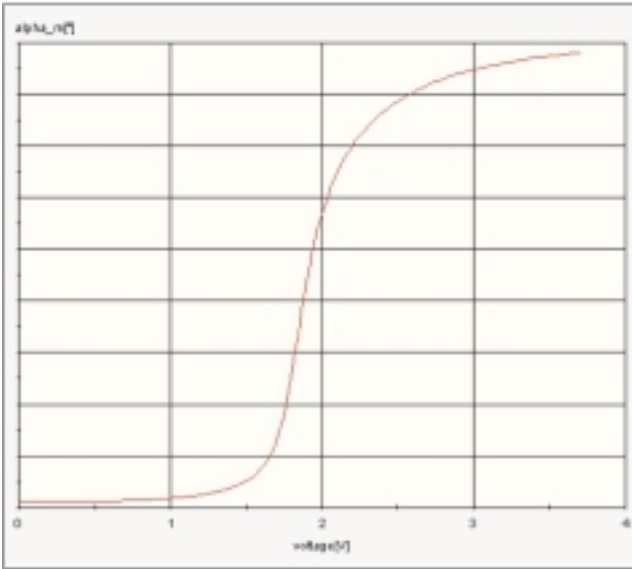


Fig. 1. Midplane tilt versus applied voltage (electro-distortional curve) of 210°-STN cell.

Director configurations with a negative slope of the curve are nonstable equilibrium states under constant voltage driving. These solutions are only accessible at constant charge across the LC-layer. This shows that the stability conditions at constant voltage and constant charge are different. It can be shown that equilibrium states stable at constant voltage are also stable at constant charge but not vice versa [22].

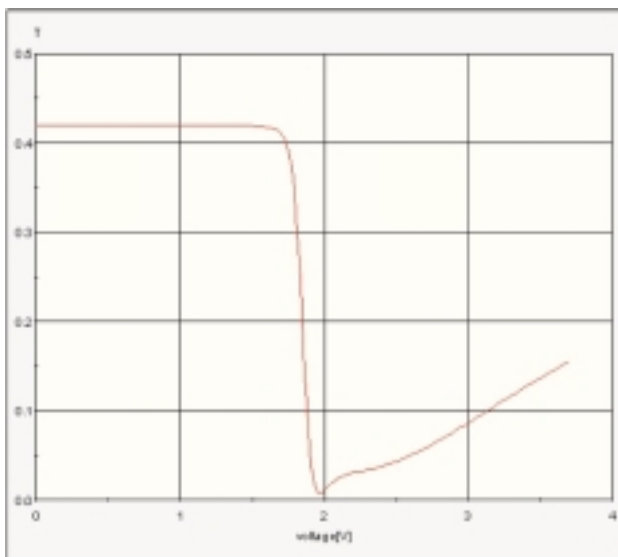


Fig. 2. Transmittance versus applied voltage (electro-optical curve) of a 210°-STN cell.

#### 4.2. Thurston’s geodesic surface

Another choice for representation of the director configuration is a mapping of the director onto a curved surface, whose shape is given by the ratio of the elastic constants  $K_{33}/K_{11}$  and  $K_{33}/K_{22}$  [23–25]. If these ratios are unity, the surface becomes

a sphere. Other ratios of the elastic constants result in deformations of the spherical shape but rotational symmetry is always maintained. The director is represented by a point on that surface so that the entire director configuration across the LC-layer becomes a path. The azimuthal position corresponds to the twist angle while the vertical position increases with the tilt angle. At 0° pretilt the path is a circular arc around the equator, since the tilt angle remains 0° throughout the LC-layer. The 90°-tilt state (i.e. homeotropic state) is mapped to north pole of the surface.

What is so special with the geodesic surface? The surface orientation on both substrates corresponds to two points on the surface. There are an infinite number of possible paths that start and end at these fixed points, but only the shortest path corresponds to a stable equilibrium state (see Fig. 3).

The geodesic surface representation allows us to check which equilibrium states are possible and whether they are stable or not. It also makes a distinct difference between topologically equivalent and not-equivalent states. All director configurations (paths) with the same end-points are topologically equivalent. Transitions between topologically nonequivalent states are only possible via discontinuities

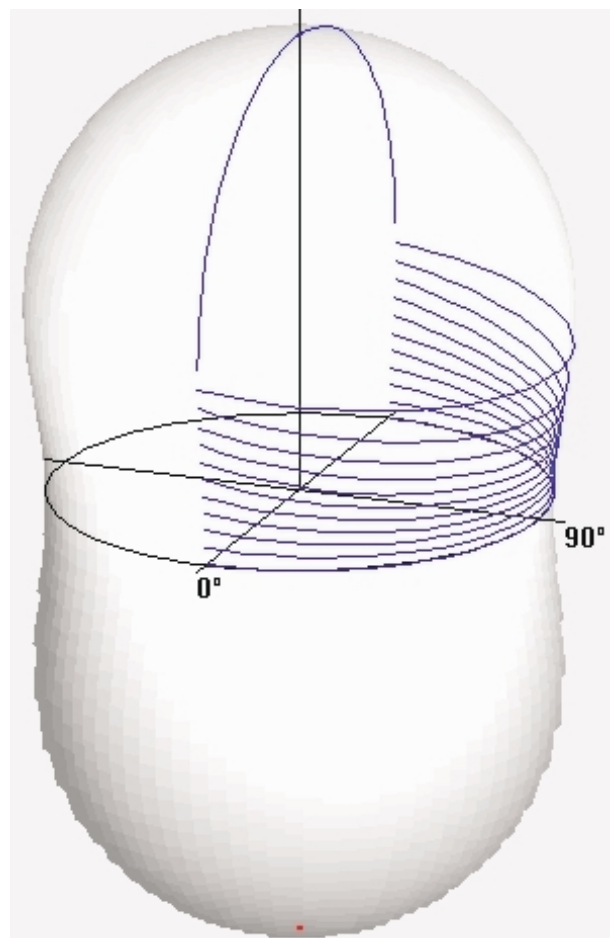


Fig. 3. Geodesic surface with stable equilibrium paths of a 180° twisted LC layer corresponding to a set of director configurations. The pretilt angle is the set parameter.

(inversion walls, other singularities). However the drawback of this representation is that the relation shortest path = stable equilibrium state does not hold when an electric field is present or when the LC is doped with chiral additives.

### 4.3. LC-optics

The optical properties of multilayered anisotropic media such as liquid crystal cells have been studied for a long time. Physical models for the optics of liquid crystals have been developed from the beginning of the century. The optics of cholesteric materials was studied by several authors like Mauguin [26], Oseen [27], and de Vries [28]. In 1941, Jones [29] published a 2×2-matrix method for calculating the optical properties of general multilayered anisotropic media at normal light incidence. 4×4 matrix methods were developed by Smith [30] and Berreman [31], which made the calculation at oblique incidence possible. Jones 2×2-matrix method was further improved by Gharadjedaghi [32] and Yeh [33] to cope with oblique incidence. Later on, other 4×4-matrix methods were developed [34,35].

These matrix methods allow the calculation of the optical properties of general birefringent multilayers with arbitrary orientation of the index ellipsoid in each layer. This flexibility made the matrix methods very attractive for the computation of LCD optics, since polarisers, retarders and of course the LC-layer itself with the arbitrary optic axis orientation can be treated in a systematic way.

There are only a few special cases where a closed form solution is known. Of practical interest are the homogeneous medium and the linearly twisted medium where the optic axis rotates linearly along the cell normal. We call these two types basic elements since the optic devices with which we are concerned here can be constructed from these elements.

The change of the polarisation state of the light wave travelling through a stack of birefringent layers can be visualised by a path on the Poincaré sphere. The path caused by the basic elements, at normal incidence, can be constructed easily. This makes the Poincaré sphere attractive for the analysis and design of LCDs with retardation foils.

### 4.4. 4×4 matrix methods

We begin with the discussion of the 4×4 matrix methods because they are more general and since they can be used as a starting point for the derivation of the 2×2 matrix methods.

**Characteristic Matrix Method.** Abeles' 2×2 characteristic matrix method [36] for isotropic media was extended for anisotropic layered media, by Smith [30], resulting in a 4×4-matrix method. Later, Teitler and Henvis and Berreman reinvented this method and applied it successfully to the simulation of the optics of LCDs [37,31]. More

recently modifications of the 4×4 characteristic matrix methods have been developed by Wöhler [40], Eidner [41], and Berreman [47,48].

For stratified media Maxwell's curl equations reduce to the following set of 4 linear differential equations of first order:

$$\frac{d\vec{\psi}}{dz} = -ik_0\Delta \cdot \vec{\psi}, \quad (6)$$

with  $k_0 = 2\pi/\lambda$  and  $\vec{\psi} = (E_x, H_y, E_y, -H_x)^T$ .  $\Delta$  is a 4×4 matrix that depends on the index ellipsoid.

The solution of Maxwell's equations for a layer can be written in the following form:

$$\vec{\psi}(z_{i+1}) = P(d_i) \cdot \vec{\psi}(z_i). \quad (7)$$

$P(d_i)$  is the characteristic 4×4 matrix which relates the tangential components of the electric and magnetic fields at levels  $z_i$  and  $z_{i+1}$  with  $d_i = z_{i+1} - z_i$ , the thickness of the layer  $i$ . A possible representation of the characteristic matrix of a single layer is given by the product of three matrices:

$$P(d) = \Psi \cdot K(d) \cdot \Psi^{-1}. \quad (8)$$

The columns of  $\Psi$  are the 4 eigenvectors of  $\Delta$  and  $K(d)$  is a diagonal matrix (propagator matrix).

The characteristic matrix of multilayered medium is given by the product of the characteristic matrices of all layers. From the characteristic matrix reflection and transmission can be calculated solving a linear equation.

**Transfer matrix method.** The transfer matrix method [34] starts at the second order wave equations. While the characteristic matrix method deals with the superposition of all partial waves, the transfer matrix method relates the weights of the eigenmodes at different locations across the LC-layer.

$$\vec{c}_{i-1}(z_{i-1}) = T_{i-1,i} \cdot \vec{c}_i(z_i) \quad (9)$$

with

$$T_{i-1,i} = \Psi_{i-1}^{-1} \cdot \Psi_i \cdot K_i^{-1}. \quad (10)$$

It should be clear that the transfer matrix  $T$  always depends on the optical parameters of two adjacent layers. The characteristic matrix on the other hand "characterises" a special layer and therefore depends only on its own optical properties. This might be very practical when optimising multilayer systems. Single layers can easily be included, removed or varied. The optical properties of adjacent layers are not needed which reduces also the overall "bookkeeping" efforts.

**Scattering matrix method.** The scattering matrix method was developed by Ko and Sambles for the study of attenuated total reflections in liquid crystals [35]. The motivation

for the development of this method was problems with numerical instabilities when strong evanescent or absorbing waves occur.

**2×2 Matrix methods.** The 4×4 matrix methods are much more complicated and the computation time is much larger compared to the 2×2 Jones matrix method. This caused several researchers to simplify the 4×4 formalism towards the Jones calculus. Gharadjedaghi developed a method for the optics at oblique incidence but his paper was hardly noticed [32]. In 1982 Yeh presented the “extended Jones matrix method” [38]. He restricted himself to the special case where the optic axis is parallel to the plane of stratification. Not before 1990 the 2×2-matrix method was re-invented by Lien [42] and Ong [43] for application to liquid crystals with arbitrary optic axis orientation. Also Gu and Yeh recently generalised their “extended Jones matrix method” [44].

The 2×2 formalism can be derived from the 4×4-matrix method by neglecting multiple reflections. This is the key to the simplification. The 4×4 method always deals with four quantities simultaneously, e.g. the four weights of the two forward and two backward propagating eigenwaves. The forward propagating waves in an arbitrary sublayer are affected by the backward propagating waves due to multiple reflections at the interfaces. This fact is expressed by a 4×4-matrix. Since all eigenwaves in all sublayers may contribute to the waves of a single sublayer the optics of a multilayer is not determined before all layers are processed. Neglecting multiple reflections decouples forward and backward propagating waves reducing the 4×4 formalism to a 2×2 calculus. The polarisation state in a sublayer is determined only by the preceding sublayers.

Another way for constructing 2×2 matrix methods is from bottom up. At the entrance of each layer the refracted wave is decomposed into two eigenwaves of the layer. With the 2×2-propagator matrix (diagonal matrix with phase terms) the eigenwaves at the exit of the medium are calculated. A further decomposition of the field vectors onto the directions parallel and perpendicular to the plane of incidence gives the two amplitudes of the light wave leaving the layer. This process is repeated for the next layers. Loss caused by reflections at each interface can be considered by using the Fresnel formulas at each interface.

**Comparison between 2×2 and 4×4 matrix methods.** The main difference between both methods is that the 2×2 formalism neglects reflections. What is the optical effect of multiple reflections? When calculating the spectrum of reflectance or transmittance for different values of e.g. the angle of incidence one may observe “high frequent” oscillations superposed to a rather smooth curve.

Most light sources used for LCD illumination have a finite bandwidth, some even being “white light” sources (no perfectly monochromatic coherent light as assumed in the computations). Moreover the thickness of the LC-layer varies slightly with the position across the layer plane. These are two reasons for measuring usually smooth curves with-

out high frequent oscillations as obtained with calculations. Thus when using 4×4 matrix methods in comparison with experimental data some kind of averaging is necessary at the cost of extra calculation time.

There are several ways to obtain “smooth curves”. A straightforward approach is to average over several wavelength values near the wavelength of the source. This is the most time consuming way. Yang eliminated most of the oscillation by matching the index of refraction of the surrounding medium (usually air) to that of the polariser’s [46]. This is a simple though very effective method since the largest difference of the refractive index is at the air-polariser interface. The single reflections of all these interfaces are calculated from the Fresnel formulas. Recently Berreman introduced apodising layers located at interfaces where large differences of the refractive index occur [47,48]. This is a less time consuming approach but it requires special care to critical layers with interfaces where the change of the index of refraction is large.

**Poincaré sphere.** The polarisation state of a light wave is determined by two parameters. One set of parameters is the ratio of the amplitudes and the phase difference. Another set is the ellipticity of the ellipse of polarisation and the angle, which specifies the orientation of the ellipse. The Stokes parameters (see e.g. [49]) as a further set are originally introduced for the study of partially polarised light.

If we restrict ourselves to lossless media and if we neglect reflections at the boundaries in the case of multilayered media, the intensity remains constant throughout the entire stack of layers. Therefore the change of polarisation can be represented by a path on a sphere (Poincaré sphere with a radius of one, see Fig. 4). The extrema of polaris-

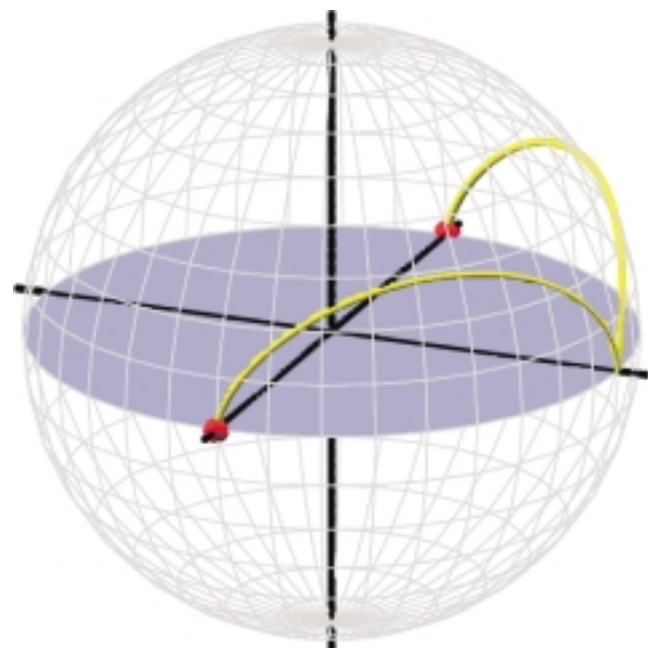


Fig. 4. Poincaré sphere with a path generated when an initially linearly polarized light wave passes through a linearly twisted layer.

ation are linearly polarised light corresponding to points on the equator and left and right-handed circularly polarised light at north and south pole respectively.

The Poincaré sphere description can be used for the design of LCDs. The effect of retardation films on the optical properties, for example, can be visualised easily and one can imagine what happens when the retardation or the orientation of the retarder is varied. Further applications of the Poincaré sphere description are the design of birefringent optical filters [51].

## 5. More-dimensional solutions

Up to now we considered one-dimensional problems where the only allowed spatial variation was along the normal to the LCD. If the pixel size becomes very small, the homogeneity along the pixel reduces and domains with different director orientations can occur. The in-plane switching effect is a typical two-dimensional problem, which can not be analysed with the above-discussed one-dimensional methods alone. The methods for the calculation of both the director configuration and the optics are much more complicated and time consuming, compared to the one-dimensional problem. As in the one-dimensional case the energy or the corresponding Euler equations must be discretised. This time however on a two- or three-dimensional grid. One can derive relaxation methods dealing with the elastic and electro-static energy. A special problem of the more dimensional case is the mutual dependence of the director orientation and the electrostatic potential distribution. A simultaneous relaxation of the director configuration and change of the potential is not possible for larger grids. A practical approximation for such a relaxation procedure is as follows:

- 1 assign initial values to the director distribution,
- 2 (with fixed director field) calculate the electro-static potential distribution,
- 3 (with fixed potential distribution) calculate a new director configuration by relaxation,
- 4 (with fixed director field) calculate the new potential distribution,
- 5 go to step 3 and repeat until (error<limit).

An alternative to that finite difference method (FDM) is the finite element method (FEM) which uses a mesh rather than a grid [52]. The mesh can be generated automatically and adapted to the geometry (LC-layer, electrodes, TFTs, etc.) more easily. Moreover it can be refined locally to assure accuracy (see Fig. 5). There exist a lot of shapes of the elements and one can mix different shapes if it is suitable for the geometry.

The calculation of the optical properties requires the solution of Maxwell's equations. One can discretise Maxwell's equations in a similar way as the Euler equations [53].

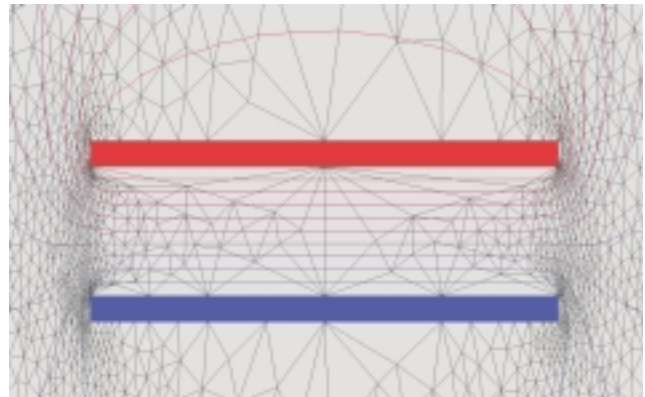


Fig. 5. Cross section of a capacitor with FEM mesh. The mesh is locally refined according to error estimates.

### 5.1. Basic problems of LCD-modelling in three dimensions

While a model of an LCD is quickly defined in one dimension (only the thickness of the layers is important besides the material parameters), a detailed cross-section through the region of interest has to be entered and edited in the two-dimensional case. After input of the geometry of the problem, the structures have to be specified with respect to their material (i.e., isotropic dielectric material, ideal electrode, liquid crystal) and with respect to the alignment properties (i.e., orientational boundary conditions and anchoring elasticity). After definition of all required aspects a suitable mesh is generated and locally refined to assure numerical accuracy. Then the initial director configuration is allowed to relax into a stable state of equilibrium before an electric field is applied to the electrodes and the director configuration relaxes into a new state of equilibrium [54].

For example, Fig. 6 shows the director configuration and the corresponding transmittance of an in-plane switching (IPS) cell in the OFF-state. When the center electrode is

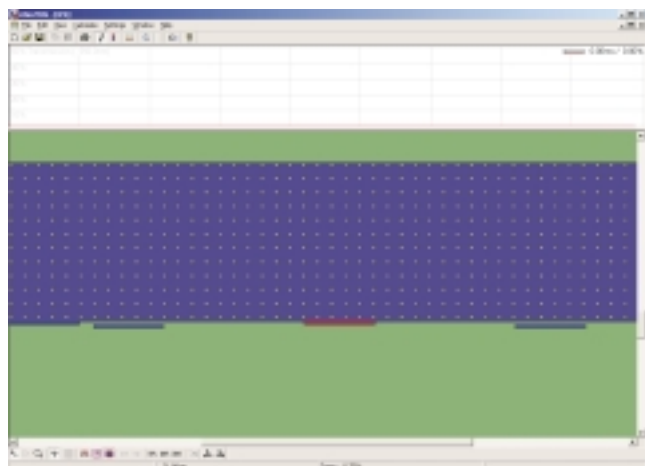


Fig. 6. Cross section of an IPS cell with electrodes at the bottom substrate in the OFF state. The directors are nearly perpendicular to the cross section.



switched ON, the directors reorientate towards the plane of the cross section. Figure 7 shows the IPS cell after 50 msec.

The problems related to definition of the geometry become even more severe in the three dimensional case; here, a complex 3D geometry editor is required together with a postprocessor for definition of material properties, alignment parameters and initial director configurations. Practical experience implies that ionic impurities in the LCD-layer may have a considerable effect on the electro-optical performance of state-of-the-art high resolution LCD-screens. In order to provide a complete model of such display devices, ionic effects should also be included in the model [55].

Finally, the number of node variables that describe the elastic and electric energy of the system increases so much that computing power and storage capacities become severe issues.

When after a certain while (depending on the power of the computer) a stable equilibrium configuration is found, it should be checked, if there are other similar configurations with a lower total energy. Once an acceptable equilibrium configuration is evaluated in three dimensions, the respective optical properties can finally be analysed. Rapid lateral variations of the nematic director (e.g. in micro-LCDs, high-resolution monitor LCDs, both with small lateral dimensions) resulting in rapid variations of the refractive index of the LC-material lead to diffraction effects which are not taken into account by optics methods for stratified media (Berreman, Jones, etc.). Alternative optics approaches are:

- finite-difference time-domain method (FDTD) (Refs. 53, 56, 57)
- (wide-angle) beam propagation method (BPM) (Ref. 58),
- (reduced-order) grating method (R-GM) (Refs. 59, 60).

Comparison of measured and calculated transmission curves (as a function of the lateral position) provides insight into details of the local director field [61] in cases of ambiguities (i.e., several stable solutions).

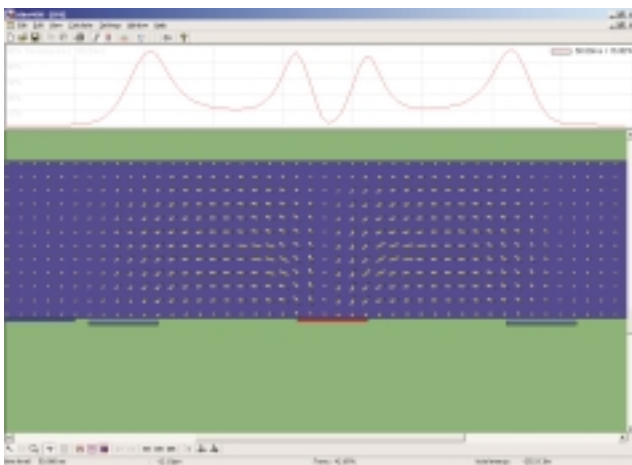


Fig. 7. Same configuration as in Fig. 6 – 50 msec after the center electrode is switched ON.

## 6. Conclusions

With increasing demand for high-quality low-price LCD-screens for both data-processing and video-applications (i.e., multimedia), numerical modelling of LCDs will be of still increasing importance for device development and optimisation in the LCD field, because of several distinct advantages over the experimental approach:

- exact and individual control of all model parameters,
- (usually) fast computation of results,
- easy optimisation of target quantities,
- simultaneous optimisation of several parameters possible,
- easy evaluation of parameter sensitivities.

However, such splendid features can only be realised when the following conditions are fulfilled:

- the model of the physical device has been set up correctly,
- the input parameters (e.g. material properties) have been measured accurately.

Two-dimensional modelling turned out to be a very helpful intermediate tool in the case of IPS-effects, but other sophisticated approaches to increase the viewing-cone (e.g. multi-domain methods) will require three-dimensional models.

Versatile three-dimensional models, however, are located on a quite different level of requirements with respect to definition of the model and its detailed properties (e.g., ionic effects may have to be considered additionally), user interaction (geometry input and assignment of properties, choice of initial director configuration), computer hardware (i.e. memory, processor speed) and software (e.g., 3d-editor).

Modelling of the detailed optical properties even of highly complex LCDs will probably remain one-dimensional also in the future due to the basic 1d-nature of most electro-optical effects (e.g., TN) and the actual drawbacks and limitations of two- and three-dimensional optics models in comparison to 1d-modeling (requirements of memory and time).

## References

1. C.Z. van Doorn, "Dynamic behavior of twisted nematic liquid-crystal layers in switched fields", *J. Appl. Phys.* **46**, 3738–3745 (1975).
2. D.W. Berreman, "Liquid-crystal twist cell dynamics with backflow", *J. Appl. Phys.* **46**, 3746–3751 (1975).
3. M.E. Becker, "DIMOS – a software tool for optimizing display systems with LCDs", *Displays* **132**, 215–228 (1989).
4. C.W. Oseen, "Beiträge zur Theorie anisotroper Flüssigkeiten", *Ark. Math. Fys.* **19A**, 1–19 (1925).
5. F.C. Frank, "On the theory of liquid crystals", *Discuss. Faraday Soc.* **25**, 19–28 (1958).
6. F.M. Leslie, *Quart. J. Mech. Anal.* **19**, 357 (1966).
7. J.L. Ericksen and J.L. Arch, *Ration. Mech. Analysis* **23**, 266 (1966).
8. J. E. Anderson *et al.*, "Shortcomings of the Q-tensor method for modeling liquid crystal devices", *SID '99 Digest*, 198 (1999).

9. D. W. Berreman, "Surface orientation and compliance effects on twist-cell performance", in *The Physics and Chemistry of Liquid Crystal Devices*, pp. 1–11, edited by C.J. Spokel, Plenum Press, New York, 1980.
10. A. Rapini and M. Papoular: "Distortion d'une lamelle nématique sous champ magnétique, conditions d'ancrage aux parois", *J. Physique* **30**, C4-54, C4-56 (1969).
11. C. Vertogen *et al.*, *Thermotropic Liquid Crystals. Fundamentals*, Springer, Berlin, 1988.
12. H. Gruler, T.J. Scheffer, and G. Meier, "Elastic constants of nematic liquid crystals I. Theory of the normal deformation", *Z. Naturforsch. A*, **27**, 966–976 (1972).
13. R.N. Thurston and D.W. Berreman, "Equilibrium and stability of liquid-crystal configurations in an electric field", *J. Appl. Phys.* **52**, 508–509 (1981).
14. M. Akatsuka *et al.*, "Film compensated STN-LCDs with wide viewing angle", *9<sup>th</sup> IDRC*, 336–339 (1989).
15. T. Miyashita *et al.*, "A wide-viewing angle color STN-LCD with biaxial retardation films", *12<sup>th</sup> IDRC*, 495–498 (1992).
16. D.W. Berreman, "Numerical modelling of twisted nematic devices", *Phil. Trans. R. Soc. Lond. A*, **309**, 203–216 (1983).
17. W.H. Press *et al.*, *Numerical Recipes in FORTRAN: The Art of Scientific Computing*, Cambridge University Press, Cambridge, 1992.
18. H. Wöhler *et al.*, "A modified Ritz method for the calculation of deformation profiles in chiral nematic liquid crystal cells", *9<sup>th</sup> IDRC*, 376–379 (1989).
19. M.E. Becker, "A new method for computing director profiles", *11<sup>th</sup> IDRC*, 503–506 (1994).
20. T.J. Scheffer and J. Nehring, "Twisted nematic and supertwisted nematic mode LCDs", in *Liquid Crystals Applications and Uses* **1**, pp. 231–274, edited by B. Bahadur, World Scientific, Singapore, 1990.
21. M.E. Becker *et al.*, "Surface-induced bistability in chiral-nematic liquid crystals: effect of liquid crystal and surface parameters", *Proc. SID*, **26**, 109–115 (1985).
22. B.N. Thurston, "Stability of nematic liquid crystal configurations", *J. Physique* **42**, 419–425 (1981).
23. R.N. Thurston and F.J. Almgren, "Liquid crystals and geodesics", *J. Physique* **42**, 413–417 (1981).
24. B.N. Thurston, "Unit sphere description of liquid-crystal configurations", *J. Appl. Phys.* **52**, 3040–3052 (1981).
25. B.N. Thurston, "Stability of nematic liquid crystal configurations", *J. Physique* **42**, 419–425 (1981).
26. M.Ch. Mauguin, "Sur les cristaux liquides de Lehmann", *Bull. Soc. Fran. Min.* **34**, 6–15 (1911).
27. C. W. Oseen, "Beiträge zur Theorie anisotroper Flüssigkeiten", *Ark. Math. Astron. Fys.* **21A**, 14–35 (1928).
28. H. de Vries, "Rotary power and other optical properties of certain liquid crystals", *Acta Crystallogr.* **4**, 219–226 (1951).
29. R. C. Jones, "A new calculus for the treatment of optical systems I. Description and discussion of the calculus", *J. Opt. Soc. Am.* **3**, 488–493 (1941).
30. D.C. Smith, "Magneto-optical scattering from multilayer magnetic and dielectric films", *Optica Acta* **12**, 13–45 (1965).
31. D.W. Berreman, "Optics in stratified and anisotropic media: 4×4-matrix formulation", *J. Opt. Soc. Am.* **62**, 502–510 (1972).
32. F. Gharadjedaghi and J. Robert, "Comportement électro-optique d'une structure nématique en hélice - application à l'affichage", *Rev. Phys. Appl.* **11**, 467–473 (1976).
33. P. Yeh, "Extended Jones matrix method", *J. Opt. Soc. Am.* **72**, 507–513 (1982).
34. P. Yeh, "Electromagnetic propagation in birefringent layered media", *J. Opt. Soc. Am.* **69**, 742–756 (1979).
35. D.Y. K. Ko and J.R. Sambles, "Scattering matrix method for propagation of radiation in stratified media: Attenuated total reflection studies of liquid crystals", *J. Opt. Soc. Am. A* **5**, 1863–1866 (1988).
36. F. Abeles: "Recherches sur la propagation des ondes électromagnétiques sinusoidales dans les milieux stratifiés. Application aux couches minces", *Anal. Phys.* **5**, 596–640 (1950).
37. S. Teitler and B. W. Hennis, "Refraction in stratified, anisotropic media", *J. Opt. Soc. Am.* **60**, 830–834 (1970).
38. D.W. Berreman, "Optics in smoothly varying planar structures: Application to liquid-crystal twist cells", *J. Opt. Soc. Am.* **63**, 1374–1380 (1973).
39. R.J. Gagnon, "Liquid-crystal twist-cell optics", *J. Opt. Soc. Am.* **71**, 348–353 (1981).
40. H. Wöhler *et al.*, "Faster 4×4 matrix method for uniaxial inhomogeneous media", *J. Opt. Soc. Am. A* **5**, 1554–1557 (1988).
41. K. Eidner *et al.*, "Optics in stratified media – the use of optical eigenmodes of uniaxial crystals in the 4×4-matrix formalism", *Mol. Cryst. Liq. Cryst.* **172**, 191–200 (1989).
42. A. Lien, "The general and simplified Jones matrix representations for the high pretilt twisted nematic cell", *J. Appl. Phys.* **67**, 2853–2856 (1990).
43. H.L. Ong: "Electro-optics of a twisted nematic liquid crystal display by 2×2 propagation matrix at oblique incidence", *Jpn. J. Appl. Phys.* **30**, L1028–L1031 (1991).
44. C. Gu and P. Yeh: "Extended Jones matrix method. II", *J. Opt. Soc. Am. A* **10**, 966–973 (1993).
45. P. Allia *et al.*, "4×4 matrix approach to chiral liquid-crystal optics", *Mol. Cryst. Liq. Cryst.* **143**, 17–29 (1987).
46. K.H. Yang, "Electro-optical properties of dual-frequency cholesteric liquid crystal reflective display and drive scheme", *J. Appl. Phys.* **68**, 1550–1554 (1990).
47. D.W. Berreman, "Ultrafast 4×4 matrix optics with averaged interference fringes", *SID 1993 Digest*, 101–104 (1993).
48. D.W. Berreman, "Quick averaging of interference fringes in 4×4 matrix optics", *Freiburger Arbeitst. Flüssigkristalle*, **25**, Freiburg (1996).
49. M. Born and E. Wolf, *Principles of Optics*, Pergamon Press, Oxford, 1980.
50. J.E. Bigelow *et al.*, "Poincare sphere analysis of liquid crystal optics", *Appl. Opt.* **16**, 2090–2096 (1977).
51. M. Johnson, "Poincare sphere representation of birefringent networks", *Appl. Opt.* **20**, 2075–2080 (1981).
52. O. Zienkiewicz *et al.*, *The Finite Element Method*, Vol.1, McGraw-Hill, New York (1994).
53. B. Witzigmann *et al.*, "Rigorous electromagnetic simulation of liquid crystal displays", *J. Opt. Soc. Am. A* **15**, 753–739 (1998).
54. M. E. Becker *et al.*, "Numerical modeling of IPS effects: A new approach and more results", *SID 1996 Digest*, 15–18 (1996).
55. H. De Vleeschouwer *et al.*, "Ion transport simulations and DC leakage current measurements in nematic LCDs", *SID 2001 Digest*, 128–131 (2001).

56. E.E. Kriezis *et al.*, “Finite-difference time domain method for lightwave propagation within liquid crystal devices“, *Opt. Comm.* **165**, 99–105 (1999).
57. C. M. Titus *et al.*, “Comparison of analytical calculations to finite-difference time-domain simulations of one-dimensional spatially varying anisotropic liquid crystal structures“, *Jap. J. Appl. Phys.* **38**, 1488–1494 (1999).
58. E. E. Kriezis *et al.*, “A wide angle beam propagation method for the analysis of tilted nematic liquid crystal structures“, *J. Mod. Opt.* **46**, 1201–1212 (1999).
59. P. Galatola *et al.*, “Symmetry properties of anisotropic dielectric gratings“, *J. Opt. Soc. Am. A* **11**, 1332–1341 (1994).
60. O.A. Peverini *et al.*, to be published.
61. D.K.G. de Boer *et al.*, “Optical simulations and measurements of in-plane switching structures with rapid refractive-index variations“, *SID 2001 Digest*, 818–821 (2001).

## Hot off the SPIE Press

### Principles of Lithography

by Harry J. Levinson, Advanced Micro Devices, Inc.

The ability to pack large numbers of individual transistors in a small area of silicon has enabled the great functionality of modern microelectronics, specifically integrated circuits. This book focuses on photolithography – the method used for patterning nearly all integrated circuits fabricated today – in which optical methods are used to transfer circuit patterns from master images, called masks or reticles, to silicon wafers.

This book can serve as an introduction to the science of microlithography for someone who is unfamiliar with the subject. The reader is expected to have a foundation in basic physics, chemistry, and elementary calculus. The text covers a number of advanced subjects and may be useful to experienced lithographers who seek a better understanding of topics outside their areas of expertise.

**Contents: Overview of lithography. Optical pattern formation. Photoresist. Modeling and thin film effects. Wafer steppers. Overlay. Masks and reticles. Overcoming the diffraction limit. Metrology. The limits of optical lithography. Lithography costs. Alternative lithography techniques. Appendix A: Coherence.**

SPIE PRESS Vol. PM97 • 410 pages

Hardcover 0-8194-4045-0 • \$58 / \$72

### Rainbows in Art, Myth, and Science

by Raymond L. Lee, Jr. and Alistair B. Fraser

Copublished with The Pennsylvania State University Press

This unique book explores the rainbow from the perspectives of atmospheric optics, art history, color theory, and mythology. Throughout history, the rainbow has been seen primarily as a symbol-of peace, covenant, or divine sanction – rather than as a natural phenomenon. The authors discuss these varied roles as they examine the rainbow's scientific, artistic, and folkloric significance.

**Contents: The bridge to the gods. Emblem and enigma. The grand ethereal bow. Optics and the daughter of wonder. Unweave a rainbow. Beyond the medieval rainbow. Color the rainbow to suit yourself. What are "All the colors of the rainbow?" The end of the bow. Sell it with a rainbow.**

SPIE PRESS Vol. PM94 • 408 pages

Hardcover 0-8194-3994-0 • \$55 / \$65

### Electroactive Polymer (EAP) Actuators as Artificial Muscles: Reality, Potential, and Challenges

Editor: Yoseph Bar-Cohen, Jet Propulsion Lab.

Electroactive polymer (EAP) materials with large displacement response are showing great potential. The ability to induce large actuation strains such as stretching, squeezing, and bending makes these resilient materials remarkably similar to biological muscles. This book describes the mechanics of natural muscles and how EAP actuators mimic their actions. It examines materials, EAP function at the

molecular level, and methods for predicting polymer response to external electric fields. The text discusses the future of EAP in robotics, entertainment, and medicine, among other industries.

**Contents: Introduction. Natural muscles. Electric EAP. Molecular EAP. Modeling electroactive polymers. Processing and fabrication of EAP. Testing and characterization. EAP actuators, devices, and mechanisms. Lesson learned, applications, and outlook.**

SPIE PRESS Vol. PM98 • 687 pages

Hardcover 0-8194-4054-X • \$70 / \$88

### Electro-Optical Imaging: System Performance and Modeling

Editor: Lucien M. Biberman, Institute for Defense Analyses

Co-published by SPIE and ONTAR Corp.

This significant compendium of technical literature traces the development of both low-light-level and infrared imaging technology, as well as system modeling and performance over the past 30 years. It presents an excellent selection of the pioneering work done here and abroad that forms the theoretical underpinnings of EO imaging. The book includes key contributions from The U.S. Army Night Vision & Electronic Sensors Directorate; Institute for Defense Analyses; Royal Aircraft Establishment, Farnborough (UK); Hughes Aircraft; Texas Instruments; Westinghouse; and RCA.

**Contents: Brief history of imaging devices for night vision. Luminance, radiance, and temperature. Natural sources of low-light-level illumination and irradiation. Early image-intensifier tube structures. Present image intensifier tube structures. Calibration and characterization of image intensifiers. Characterization and calibration of signal-generating image sensors. Thermal imaging sensors. Characterization of infrared imaging devices. Atmospheric transmission. Alternate modeling concepts. Modeling the performance of imaging sensors. Static performance model based on the perfect synchronous integrator model. Synthesis and analysis of imaging sensors. Modeling parameters for target identification: a critical features analysis. Assessing target detection models. Modeling the observer in target acquisition. Modeling false alarms in target acquisition. Low-light-level performance of visual systems. Bandwidth and Foveal vision: factors affecting the performance of image intensifier systems. Visual detection process for electro-optical images: man – the final stage of an electrooptical imaging system. System performance and image quality. Image reproduction by a line raster process. The aliasing problems in two-dimensional sampled imagery. Display of sampled imagery. Sensor system psychophysics. Visual psychophysics of head-mounted displays. Characterization of backgrounds. Weather, season, geography, and imaging system performance. Neoclassic model for search.**

SPIE PRESS Vol. PM96 • 1220 pages

Hardcover 0-8194-3999-1 • \$95 / \$115